

Global Sensitivity Analysis of a Microbial Fuel Cell Model

Yankai Yin¹, Chengcai Fu², Fengying Ma^{1,*}

¹ School of Electrical Engineering and Automation, Qilu University of Technology, Jinan 250100, P R China

² School of Mechanical Electronic & Information Engineering, China University of Mining & Technology, Beijing 100083, P R China

*E-mail: mafengy@163.com

Received: 7 April 2019 / Accepted: 7 September 2019 / Published: 7 October 2019

The global sensitivity method based on variance was applied to the microbial fuel cell (MFC) field for the first time here. The purpose of this study was to expound how the global sensitivity method can be used in the mathematical model of MFC and to visualize the sensitivity index of eight key parameters, such as the flow rate of the fuel feed, with respect to the MFC power performance. This algorithm can not only clarify the influence of uncertain parameters on power density, but also explain the influence of the interaction of uncertain parameters on MFC power density. The result shows that the cathodic charge transfer coefficient, acetate concentration in the influent of the anode chamber, forward rate constant of anode reaction under standard conditions, half velocity rate constant for acetate, charge transfer coefficient of the anode, forward rate constant of the cathode reaction under standard conditions and flow rate of the fuel feed to the anode are sensitive parameters that affect the power density of MFC; furthermore, the cathodic charge transfer coefficient is the most influential. Additionally, it was found that the electrical conductivity of the aqueous solution in MFC is the least sensitive parameter. The research achievements in this paper can be used in model optimization, parameter analysis or model simplification.

Keywords: global sensitivity; microbial fuel cell; variance-based method; electrochemical model

1. INTRODUCTION

Economic development has led to a growing contradiction between environment and energy, and the development of green renewable energy will be widely concerned. Microbial fuel cell (MFC) technology has developed rapidly over the last few years as a result of its potential applications in pollution treatment, ecological restoration and power generation [1-7]. Under mild operating conditions, MFC produce electrical energy by oxidizing organic matter in the presence of fermenting bacteria [8]. The potential (biologically mediated) generated by bacterial activity (the series of redox reactions that

produce protons (H^+) and electrons (e^-) and electron acceptor conditions produces bioelectricity [4]. Microorganisms extract energy from oxidation-reduction reactions (catabolism) to produce biomass (an anabolic process) under electron donor/receptor conditions [9].

However, many restrictions hinder the widespread use of MFCs. More importantly, the power density of MFC is lower than that of other fuel cells, so the technology has remained in the laboratory stage [10,11]. In the past few years, the pharmacological activity of microbial communities and electrode modification is the main tendency of MFC biology. The first-rank experimental conditions can be determined either by a large number of laboratory experiments or by a mathematical model. Model alternatives are more advantageous than experimental ones because they take less time and cost to obtain the desired results. In addition, different designs and configurations of MFC have been proposed [12-15]. Pinta et al. [16-18] established the MFC incentive model and optimized the power performance. In 2010, Lorenzo et al. found a positive correlation between the anode surface area and the output current density in MFC [19]. Based on experimental analysis, Ren et al. [20] proposed that smaller MFCs have a higher current density and power density than do larger MFC. Cheng et al. [21] found that the output of the system increased with increasing anode substrate concentration and cathode solution conductivity. Alavijeh et al. [22] combined the diffusion effect of matrix on biofilm and the competition of biofilm in the same substrate, proposed an equation for MFCs wastewater treatment. Ou et al. [23] proposed a one-dimensional transient model of single-chamber MFC without considering the change of cathode biofilm thickness and concentration distribution in biofilm area. Katuri et al. [24] calculated the current density by introducing the basic Butler-Volmer equation, and expressed the overpotential of the anode with the hyperbolic sinusoidal function. On the basis of mass balance, a simple expression of anode steady-state overpotential was derived. Cheng et al. [25-26] studied the effects of MFC size, anode feed flow rate and quantity of electricity-producing bacteria in the feed flow rate on power generation. Based on experimental, Picioreanu et al. [27-28] computationally simulated the variation in current, voltage, substrate concentration and microorganisms with time under different conditions.

Calculation method plays a critical role in the development of fuel cells and has the preferable performance under various operating conditions. As a matter of fact, modelling or computational methods are tools for conducting simulation experiments that require complex operations and are costly, such as material studies, complex geometries, and steady-state and dynamic fuel cell characteristics [29,30]. Computational approaches can bridge knowledge gaps, thereby achieving better performance and discovering new possibilities for optimizing MFC operation. The main difficulty in obtaining accurate MFC dynamic models is the absence of information concerning the exact values applied to model parameters. The analysis and selection of parameters can significantly impact the MFC power generation. To obtain better model predictions and higher accuracy, it is necessary to apply evaluation methods to quantify the uncertainty or confidence of the estimated parameters. Sensitivity analysis (SA) is an important means for obtaining better model and measuring the quality of parameter estimates [31-33]. SA can show the impact on the system of univariate or multivariate changes [34]. Saltelli et al. [31] consider SA to be an assessment of the extent to which each input parameter affects output uncertainty. The analysis method of SA is to generate the value of the factor on the basis of mathematical rules, and then calculate the output corresponding to the mathematical model. The result obtained from SA allows for the changes in the outputs to be mapped in light of the variability of the input parameters [35].

Additionally, SA can also be used to discover technical defects in a model, identify the key areas of input, discern the priority of research, simplify a model and so on [36]. Song et al. [33] reviewed the common methods and application areas of SA. Saltelli et al. [37] concentrated on the application of SA in chemical models. Borgonovo et al. [38] studied the measures of uncertainty and sensitivity and Perz et al. [39] summarized the global sensitivity analysis (GSA) and uncertainty analysis (UA) methods applied to ecological resilience. Although global sensitivity analysis is used in different fields of science, the method used in the fuel cell field has rarely been studied [40]. For example, Li et al. [41] established a dimensionless steady-state calculation model for a fuel cells and evaluated the influence of various parameters on outputs using multi-parameter sensitivity analysis (MPSA) based on this model. Srinivasulu et al. [42] focused on the sensitivity investigation of proton exchange membrane fuel cell (PEMFC) electrochemical model by using MPSA and aimed to determine the extent to which each parameter affects the modelling results.

MPSA is a regionalized sensitivity analysis (RSA). The advantage of regionalized sensitivity analysis lies in the small number of calculations required, but in order to obtain a more accurate evaluation of parameter sensitivity, the current research is more inclined to use the global sensitivity analysis method [43]. Laoun et al. [35] proposed the method of applying the variance-enhanced global sensitivity technique to the PEMFC model. Baroni et al. [44] proposed a general probabilistic framework for uncertainty and global sensitivity analysis of hydrological model, and based on this, first-order sensitivity indices and total sensitivity indices were estimated. Based on the Rothermel equations, an analysis of scale effects and a global sensitivity analysis have been presented by Salvador et al. The results of the GSA indicated the tiny effect of the changeability of the low heat content, the particle density and the mineral content on the outputs. However, all other input variables had some obvious effects on the output, which cannot be neglected [45]. Nossent et al. [46] presented a result of the global sensitivity analysis for flow simulations of a Soil-Water-Atmosphere-Plant (SWAT) model. By using a model-independent Sobol' method, some major shortcomings of screening sensitivity analysis methods commonly used in SWAT are overcome. The purpose of this paper was to use the variance-based global sensitivity analysis method to compute the sensitivity index of key parameters in the MFC model for the first time in the MFC field. Using this method, we can obtain a more comprehensive understanding of the overall impact of the changes in multiple parameters on the MFC output. This paper is structured in the following order: Section 2 gives a brief review to the typical continuous flow microbial fuel cell model; Section 3 describes the mathematical methods used for the GSA method; and Section 4 presents the performance tests and simulation results. Finally, the conclusions are presented at the end of this paper.

2. MFC MODELLING DESCRIPTION

A typical microbial fuel cell consist of two reaction chambers. A schematic diagram of an MFC system is shown in Fig. 1. There are two kinds of reactions in MFC: electrochemical and biochemical [47]. Electrochemical reactions involve the electron transfer and the generation of energy, the biochemical reactions involve microbial metabolism and the reduction of organic matter. The primary

transfer processes of matter, electrons and protons in typical microbial fuel cells are as follows [48]:

1. The organic matter in the anode chamber reacts on the active surface of the microorganism, releasing protons and electrons.
2. Electrons transfer to the electrode surface through the microbial cell membrane.
3. The electrons are transferred to the cathode through an external circuit.
4. Protons in the anode chamber are transferred to the cathode chamber by the proton exchange membrane.
5. The electron acceptor in the cathode chamber is transferred from the solution to the electrode surface.
6. The cathode electron acceptor permeates the cathode chamber to the anode.
7. The fuel (organic matter) in the anode chamber is transferred to the active surface of the microorganism via the host matrix.

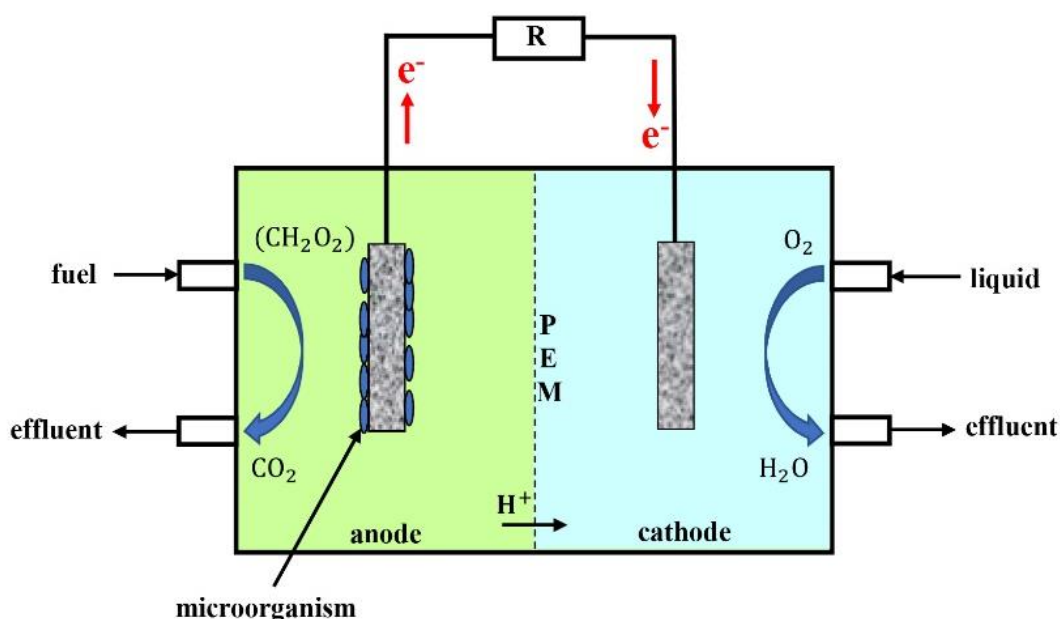
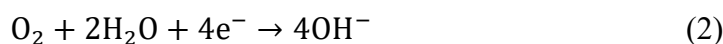


Figure 1. Schematic diagram of an MFC system

This paper focuses on the effects of various MFC parameters on generation of electrical energy by microorganisms; thus, a two-compartment MFC mathematical model was adopted. In this section, a mathematical model for studying the power generation of microbial fuel cells is introduced in detail based on literature [48].

The basic electrochemical reactions are given as follows:



The anode chamber operated under anoxic conditions, and the Monod-type equation was used to describe the anodic reaction rate (r_1). The reaction rate of the anode chamber is described as follows:

$$r_1 = k_1^0 \exp\left(\frac{\alpha F}{RT} \eta_a\right) \frac{C_{AC}}{K_{AC} + C_{AC}} X \tag{3}$$

where C_{AC} is the concentration of acetate, X denotes the biomass in the anode compartment, η_a is the anodic polarization overpotential, K_{AC} represents the half velocity rate constant for acetate, α denote the charge transfer coefficient of the anodic reaction, k_1^0 is the rate constant of the anodic reaction under standard conditions, F denotes the Faraday constant, T is the cell operating temperature, and R is the gas constant.

The Butler-Volmer expression was used to describe the electrochemical reaction. The reaction rate of the cathode chamber is given as:

$$r_2 = -k_2^0 \frac{C_{O_2}}{K_{O_2} + C_{O_2}} \exp \left[(\beta - 1) \frac{F}{RT} \eta_c \right] \quad (4)$$

where η_c is the overpotential at the cathode, C_{O_2} denotes the concentration of the dissolved oxygen, β is the charge-transfer coefficient, k_2^0 represents the rate constant of the cathodic reaction under standard conditions, and K_{O_2} is the half-velocity rate constant for dissolved oxygen.

The anode and cathode chambers of the MFC system are regarded as a continuous reactor, and four mass balance equations for the acetate, dissolved CO_2 , hydrogen ion and biomass in the anode chamber were obtained, respectively, and are defined as follows:

$$V_a \frac{dC_{AC}}{dt} = Q_a (C_{AC}^{in} - C_{AC}) - A_m r_1 \quad (5)$$

$$V_a \frac{dC_{CO_2}}{dt} = Q_a (C_{CO_2}^{in} - C_{CO_2}) + 2A_m r_1 \quad (6)$$

$$V_a \frac{dC_H}{dt} = Q_a (C_H^{in} - C_H) + 8A_m r_1 \quad (7)$$

$$V_a \frac{dC_X}{dt} = Q_a \left(\frac{X^{in} - X}{f_x} \right) + A_m Y_{ac} r_1 - V_a K_{dec} X \quad (8)$$

where subscript 'a' and superscript 'in' represent the anode and flow of feed, respectively; V , Q and A_m denote the volume, the flow rate and the cross-section area of the membrane, respectively; and Y_{ac} , f_x , and K_{dec} are the bacterial yield, the reciprocal of the wash-out fraction and the decay constant for acetate utilizers, respectively.

The same method was used to obtain three mass balance equations for the dissolved oxygen, hydroxyls, and M^+ ions in the cathode chamber, which are written as:

$$V_c \frac{dC_{O_2}}{dt} = Q_c (C_{O_2}^{in} - C_{O_2}) + A_m r_2 \quad (9)$$

$$V_c \frac{dC_{OH}}{dt} = Q_c (C_{OH}^{in} - C_{OH}) - 4A_m r_2 \quad (10)$$

$$V_c \frac{dC_M}{dt} = Q_c (C_M^{in} - C_{O_2}) + A_m N_M \quad (11)$$

where the subscript 'c' refers to the cathode and N_M stands for the flow of M^+ ions through the membrane, which can be calculated as follows:

$$N_M = \frac{3600 i_{cell}}{F} \quad (12)$$

The charge balances at the anode and cathode are described as follows:

$$C_a \frac{d\eta_a}{dt} = 3600 i_{cell} - 8F r_1 \quad (13)$$

$$C_c \frac{d\eta_c}{dt} = 3600 i_{cell} + 4F r_2 \quad (14)$$

where i_{cell} denotes the cell current density, C_a and C_c denote the anode capacitance and cathode capacitance, respectively.

The output voltage of the cell is expressed as follows:

$$V_{cell} = V_0 - \eta_a + \eta_c - \left(\frac{d^m}{k^m} + \frac{d^{cell}}{k^{aq}} \right) i_{cell} \quad (15)$$

where V_0 represents the open-circuit voltage, d_m is the membrane thickness, d_{cell} denotes the electrode distance, k_{aq} is the conductivity of the solution, and k_m is the conductivity of the membrane.

The meanings and standard values of the parameters in the model are shown in Table 1.

Table 1. Nominal values of parameters for the MFC model

Description	Symbol/Unit	Value
Flow rate of fuel feed to anode	$Q_a/\text{m}^3 \text{ h}^{-1}$	2.25×10^{-5}
Flow rate of feed to cathode compartment	$Q_c/\text{m}^3 \text{ h}^{-1}$	1.11×10^{-3}
Concentration of acetate in the influent of anode compartment	$C_{AC}^{in}/\text{mol m}^{-3}$	1.56
Concentration of CO_2 in the influent of anode compartment	$C_{\text{CO}_2}^{in}/\text{mol m}^{-3}$	0
Concentration of bacteria in the influent of anode compartment	$X^{in}/\text{mol m}^{-3}$	0
Concentration of H^+ in the influent of anode compartment	$C_H^{in}/\text{mol m}^{-3}$	0
Concentration of dissolved O_2 in the influent of cathode compartment	$C_{\text{O}_2}^{in}/\text{mol m}^{-3}$	0.3125
Concentration of M^+ in the influent of cathode compartment	$C_M^{in}/\text{mol m}^{-3}$	0
Concentration of OH^- in the influent of cathode compartment	$C_{\text{OH}}^{in}/\text{mol m}^{-3}$	0
Faraday's constant	$F/\text{Coulombs mol}^{-1}$	96485.4
Gas constant	$R/\text{J mol}^{-1} \text{ K}^{-1}$	8.3144
Temperature	T/K	303
Electrical conductivity of membrane	$k^m/\text{Ohm}^{-1} \text{ m}^{-1}$	17
Thickness of membrane	d^m/m	1.778×10^{-4}
Electrical conductivity of the aqueous solution	$k^{aq}/\text{Ohm}^{-1} \text{ m}^{-1}$	5
Distance between anode and cathode in the cell	d^{cell}/m	2.2×10^{-2}
Capacitance of anode	$C_a/\text{F m}^{-2}$	4×10^2
Capacitance of cathode	$C_c/\text{F m}^{-2}$	5×10^2
Volume of anode compartment	V_a/m^3	5.5×10^{-5}
Volume of cathode compartment	V_c/m^3	5.5×10^{-5}
Area of membrane	A_m/m^2	5×10^{-4}
Bacterial yield	$Y_{ac}/\text{Dimensionless}$	0.05
Decay constant for acetate	K_{dec}/h^{-1}	8.33×10^{-4}
Reciprocal of wash-out fraction	$f_x/\text{Dimensionless}$	10
Cell open circuit potential	V_0/volt	0.77
Forward rate constant of anode reaction under standard conditions	$k_1^0/\text{mol m}^{-2} \text{ h}^{-1}$	0.207
Forward rate constant of cathode reaction under standard conditions	$k_2^0/\text{m}^{12} \text{ mol}^{-4} \text{ h}^{-1}$	3.288×10^{-5}
Half velocity rate constant for acetate	$K_{AC}/\text{mol m}^{-3}$	0.592
Half velocity rate constant for dissolved oxygen	$K_{\text{O}_2}/\text{mol m}^{-3}$	0.004
Charge transfer coefficient of anode	$\alpha/\text{Dimensionless}$	0.051
Charge transfer coefficient of cathode	$\beta/\text{Dimensionless}$	0.663

3. GLOBAL SENSITIVITY ANALYSIS

Usually, when parameters are known to affect the output of the mathematical model, we may use the technical terminology ‘sensitive’, ‘more important’, ‘primary’ or ‘effective’ interchangeably [49]. Saltelli et al. [31] defined SA as the method of how to assign variation in statistical model outputs to different changes in model inputs. Thabane et al. [50] consider SA as a suitable way to solve the problem of ‘What happens to the results if the key inputs or assumptions change?’. Sensitivity analysis is divided into two categories: local sensitivity analysis (LSA) and global sensitivity analysis. LSA is an analysis of small range variations of a single input parameter, whereas GSA is focused on the influences of multiparameter over the whole input space [51].

3.1 Sensitivity index estimation

The global sensitivity index based on variance decomposition analysis proposed by Sobol [52] in 1993 has become an milestone in the global sensitivity analysis method, and it has been supplemented and developed by Homma and Saltelli [53]. Based on Sobol’s research, the concept of gross effect of input random variables was proposed, and it further improved the global sensitivity analysis system based on variance.

The details of GSA method are described as follows:

$$Y_{output} = f(X_1, X_2, \dots, X_k) \tag{16}$$

where Y_{output} represents the expected outputs, f is the model function and X_1, X_2, \dots, X_k are the parameters that influence the outputs.

The first-order coefficient can be calculated as follows:

$$S_i = \frac{Var_{X_i}(E_{X \sim i}(Y_{output}|X_i))}{Var(Y_{output})} \tag{17}$$

The total effect sensitivity analysis can be described as follows:

$$S_{T_i} = 1 - \frac{Var_{X \sim i}(E_{X_i}(Y_{output}|X \sim i))}{Var(Y_{output})} = \frac{E_{X \sim i}(Var_{X_i}(Y_{output}|X \sim i))}{Var(Y_{output})} \tag{18}$$

where X_i represents a matrix of all factors, $X \sim i$ is a matrix of all factors except for the factor X_i , $Var_{X_i}(\cdot)$ and $E_{X_i}(\cdot)$ represent the variance and mean of argument (\cdot) taken over X_i , and $Var_{X \sim i}(\cdot)$ and $E_{X \sim i}(\cdot)$ stand for the variance and mean of argument (\cdot) , including all factors except for X_i .

To apply GSA, the steps to obtain the input data are as follows:

1. Select the parameters you want to test.
2. Set a change interval for each parameter.
3. Within each parameter range, generate a sample that obeys the Sobol sequence, with the number of samples per parameter being N .
4. Generate the matrices $A, B, A_B^{(i)}$ of each k parameter.

The calculation methods of $Var_{X_i}(\cdot)$ and $E_{X \sim i}(\cdot)$ are as follows:

$$Var_{X_i}(E_{X \sim i}(Y_{output}|X_i)) \approx \frac{1}{N} \sum_{j=1}^N f(B)_j \left(f(A_B^{(i)})_j - f(A)_j \right) \tag{19}$$

$$E_{X \sim i}(Var_{X_i}(Y_{output}|X \sim i)) \approx \frac{1}{2N} \sum_{j=1}^N \left(f(A)_j - f(A_B^{(i)})_j \right)^2 \tag{20}$$

where A and B are design matrices of size $N \times k$; the column i in matrix $A_B^{(i)}$ is selected from matrix B , and other $k - 1$ columns are selected from matrix A . f denotes the evaluation of the function in the design matrix. The settings of matrices A and B can be obtained from references [54] and [55].

4. RESULTS AND DISCUSSION BASED ON MFC MODEL

This section focuses on how GSA is applied to the MFC mathematical model and evaluates the effects of input parameters on the output under steady and dynamic conditions. By introducing the model, we can conclude that a number of parameters in the model may have an impact on the output, and we choose the most representative parameters for research: the forward rate constant of an anodic reaction under standard conditions (k_1^0), the half velocity rate constant for acetate (K_{AC}), the forward rate constant of an cathodic reaction under standard conditions (k_2^0), the anodic charge transfer coefficient (α), the cathodic charge transfer coefficient (β), the concentration of acetate in the influent of the anode compartment (C_{AC}^{in}), the flow rate of the fuel feed to the anode (Q_a) and the electrical conductivity of the aqueous solution (k^{aq}).

First, the initial value of parameters during the execution of the program was obtained from Table 1, and the initial value was set to the centre value. In the process of model simulation, the range of parameters needed for MFC was determined. Sobol sequences were generated at different ranges for all parameters and the number of sampling points was set as 3000. The variation range of the parameters as shown in Table 2.

Table 2. Range of selected parameters for the sensitivity analysis

Symbol/Unit	Centre value	Lower limit	Upper limit
$k_1^0/\text{mol m}^{-2} \text{h}^{-1}$	0.207	0.1656	0.2484
$K_{AC}/\text{mol m}^{-3}$	0.592	0.4736	0.7104
$k_2^0/\text{m}^{12} \text{mol}^{-4} \text{h}^{-1}$	0.00003288	0.0000263	0.000039456
$\alpha/\text{Dimensionless}$	0.051	0.0408	0.0612
$\beta/\text{Dimensionless}$	0.663	0.5304	0.7956
$C_{AC}^{in}/\text{mol m}^{-3}$	1.56	1.248	1.872
$Q_a/\text{m}^3 \text{h}^{-1}$	0.0000225	0.000018	0.000027
$k^{aq}/\text{Ohm}^{-1} \text{m}^{-1}$	5	4	6

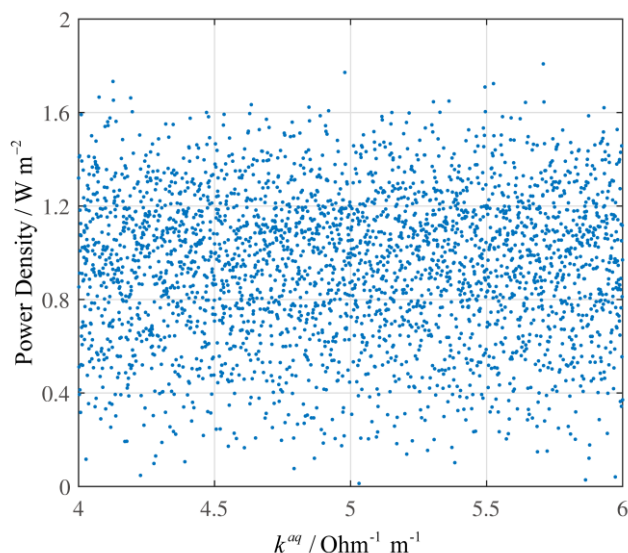


Figure 2. Dependence of MFC power density on the electrical conductivity of the aqueous solution

The parameters were evaluated by GSA method, and each parameter was represented by a scatterplot to show its effect on the power density. The scatterplots of the MFC power density versus the electrical conductivity of the aqueous solution is shown in Fig. 2. From the diagram, we can conclude that the power density is insensitive to k^{aq} within the range of 4 to 6 $\text{Ohm}^{-1} \text{m}^{-1}$, and exhibits weak discernible patterns. This phenomenon indicates that the research emphasis should be placed elsewhere and studying the effects of k^{aq} on power density should be avoided.

The diagram of the MFC power density versus the half velocity rate constant for acetate, the forward rate constant of the cathodic reaction under standard conditions, the anodic charge transfer coefficient and the concentration of acetate in the influent of the anode compartment are shown in Fig. 3. From these figures, we can conclude that these four parameters exhibit discernible weak linear patterns compared to the k^{aq} . This conclusion suggests that changes in these parameters have an impact on the power density. The power density increases slightly as C_{AC}^{in} and k_2^0 increases, and decreases as K_{AC} and α increases. During the experiment, researchers can appropriately increase the value of anode chamber acetate feed concentration to get higher power density.

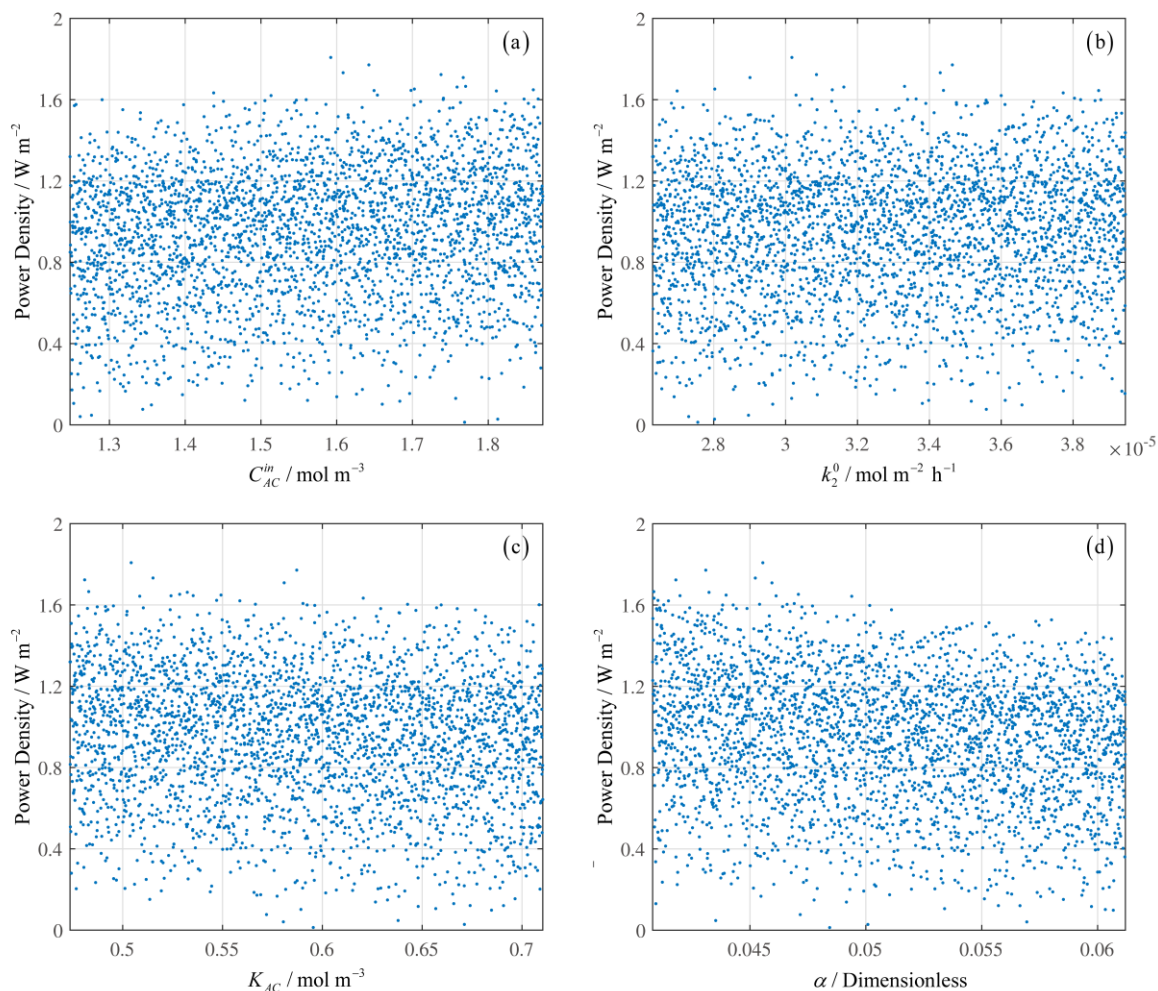


Figure 3. Dependence of MFC power density on the (a) concentration of acetate in the influent of the anode compartment, (b) forward rate constant of the cathode reaction under standard conditions, (c) half velocity rate constant for acetate and (d) anodic charge transfer coefficient

The scatterplots, shown in Fig. 4, exhibit discernible strong linear patterns, which indicate that the power density is sensitive to the forward rate constant of the anodic reaction under standard conditions and the flow rate of fuel feed to the anode. The results indicate that k_1^0 and Q_a are control variables, where k_1^0 is positively correlated with the power density and Q_a is negatively correlated with the power density. When k_1^0 changes from 0.1656 to 0.2484 mol m⁻² h⁻¹, the power density increases by 0.4 W m⁻² accordingly. In contrast, when Q_a changes from 0.000018 to 0.000027, the power density shows a downward trend. Based on above analysis, we believe that an increased flow rate supply to the anode may slow down the biochemical reaction and reduce the power generation when other factors tend toward the extreme value.

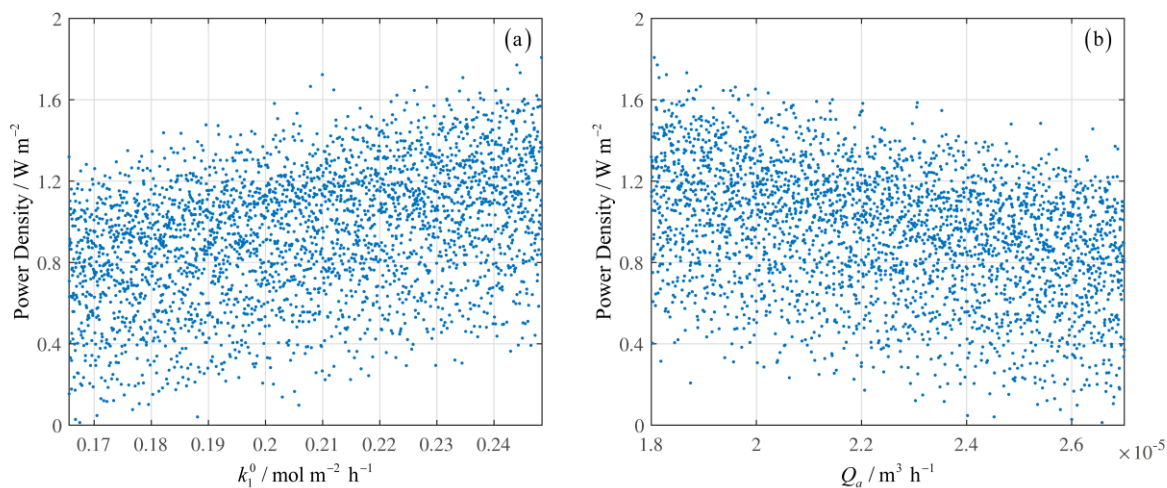


Figure 4. Dependence of MFC power density on the (a) forward rate constant of the anodic reaction under standard conditions and the (b) flow rate of the fuel feed to the anode

The result of the MFC power density versus the cathodic charge transfer coefficient within the range of 0.5304 and 0.7956 is shown in Fig. 5. The scatterplot exhibits a discernible nonlinear pattern suggesting that β is the control variable. The geometrical shape clearly states the noticeable effect of the change of the β on the outputs. Within the range of β , the value range of power density changes from 0.8-1.6 W m⁻² to 0-0.8 W m⁻².

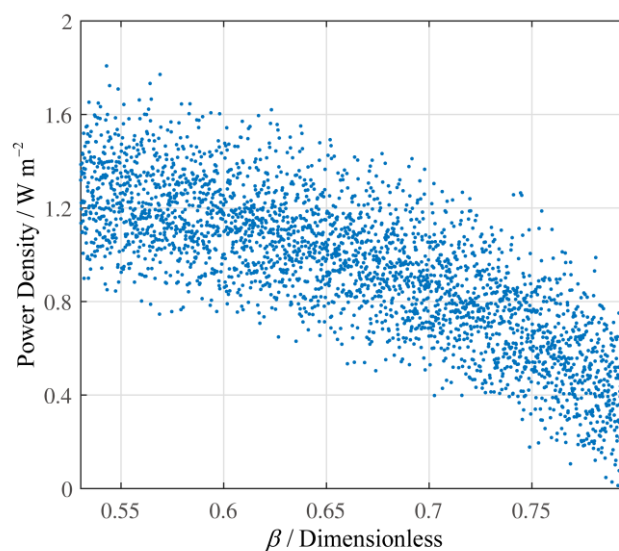


Figure 5. Dependence of MFC power density on the cathodic charge transfer coefficient

The first-order sensitivity coefficient based on variance reflects the degree of influence on the MFC output when variables act alone, and the total sensitivity represent the degree of influence on the MFC output considering the cross-action of variables. The higher the sensitivity of variables in the parameters, the sensitivity coefficient is closer to 1. The first-order sensitivities and total sensitivities of the model were calculated by Equation 17 and Equation 18, and are shown in Table 3. From Table 3, we

can determine the sequence of first-order sensitivity: charge transfer coefficient of the cathode, forward rate constant of the anodic reaction under standard conditions, flow rate of the fuel feed to the anode, anodic charge transfer coefficient, concentration of acetate in the influent of the anode compartment, half velocity rate constant for acetate, forward rate constant of the cathode reaction under standard conditions, and electrical conductivity of the aqueous solution. The sequence of total sensitivity was the same as that for first-order sensitivities. The histogram of first-order and total sensitivity is shown in Fig. 6. We can see more intuitively that the sensitivity of the electrical conductivity of the aqueous solution is almost zero which shows that there is almost no interaction between this parameter with other parameters. The first-order sensitivity and the total sensitivity of β are greater than those of other parameters, which play a decisive role in the power generation of the model. The difference between the first-order sensitivity and the total sensitivity reflects the interaction between the variable and other variables. A large difference indicates that the parameter has a greater impact on the system when the parameter changes with other variables. The difference between the total sensitivity and the first-order sensitivity of each parameter is shown in Table 3 and Fig. 6. These indicate that different parameters change at the same time, i.e., the output power under more complex experimental conditions is only slightly different from that under a single experimental condition. It also shows that only a certain parameter or a combination of specific parameters can cause a large change in the power density.

Table 3. First-order effects and total effects of the parameters

Factor/Unit	First-order effect	Total effect	Difference value
$k_1^0/\text{mol m}^{-2} \text{h}^{-1}$	0.1505	0.1517	0.0012
$K_{AC}/\text{mol m}^{-3}$	0.0149	0.0155	0.0006
$k_2^0/\text{mol m}^{-2} \text{h}^{-1}$	0.0030	0.0046	0.0016
$\alpha/\text{Dimensionless}$	0.0286	0.0342	0.0056
$\beta/\text{Dimensionless}$	0.6528	0.6543	0.0015
$C_{AC}^{in}/\text{mol m}^{-3}$	0.0191	0.0214	0.0023
$Q_a/\text{m}^3 \text{h}^{-1}$	0.1269	0.1279	0.001
$k^{aq}/\text{Ohm}^{-1} \text{m}^{-1}$	3.3603×10^{-4}	0.0018	1.46397×10^{-3}

Through analysing the above images and data, we classify the effects of all parameters on power density. Among them, β has a strong nonlinear influence, k_1^0 and Q_a have a strong linear effect, C_{AC}^{in} , k_2^0 , K_{AC} and α have a weak linear effect, and k^{aq} has no significant influence. At the same time, these data and graphs also illustrate the ability of GSA analyse the MFC mathematical model. For example, the results in the literature [56] clearly demonstrate that the greater the anode feed flow rate at the same current density is, the lower the power density of the output. To improve the power density of MFC, one of the most important solutions is to adjust the anode feed flow reasonably, but this is beyond the scope of this research, and should become the research emphasis of MFC performance optimization. Additionally, as observed by authors [48] the higher the concentration of acetate in the influent of the anode compartment is, the better the MFC power generation becomes, adequate substrate concentration provides continuous nutrients for microbial redox reactions that occurs in the microbial fuel cells. Each

point in Fig. 2 to Fig. 5 represents a different situation that may occur during the course of an experiment. Compared with the local sensitivity analysis method used in the literature [48], the GSA method used in this paper can illustrate the effect of uncertain parameters on the output more clearly. By calculating and comparing the first-order sensitivity index with the total sensitivity index, the cross-influence between one uncertain parameter and other uncertain parameters can be understood more deeply.

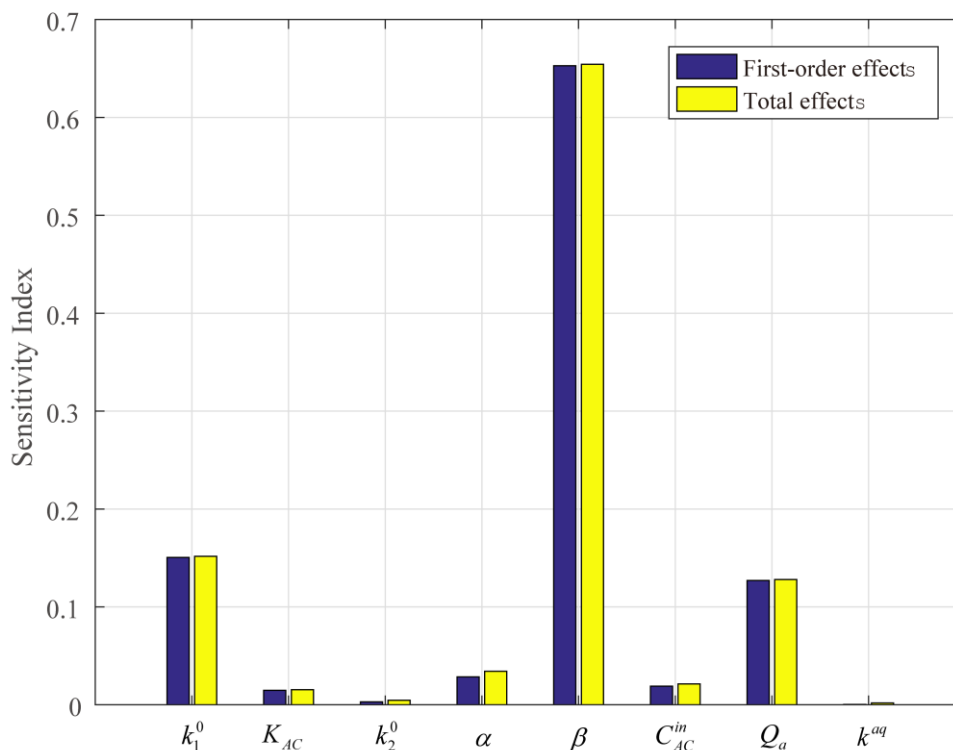


Figure 6. Sensitivity indices for the first-order effects and total effects of the parameters

5. CONCLUSIONS

First, this paper presents a variance-based global sensitivity analysis method and introduces it to the microbial fuel cell model analysis for the first time. Additionally, based on the MFC model, an analysis system for microbial fuel cells was established using the following parameters: charge transfer coefficient of the cathode, forward rate constant of the anodic reaction under standard conditions, flow rate of the fuel feed to the anode, anodic charge transfer coefficient, concentration of acetate in the influent of the anode compartment, half velocity rate constant for acetate, forward rate constant of the cathode reaction and electrical conductivity of the aqueous solution. Taking into consideration the optimization of MFC, this paper focuses on the effect of different parameters on the power density. The analysis results show that the cathodic charge transfer coefficient had the greatest effect on the power density, while the electrical conductivity of the aqueous solution had almost no effect on the results. Above all, it can be concluded that even the number of model evaluations is limited, the global sensitivity

analysis can be successfully applied for parameter analysis and parameter optimization in consideration of the input parameters of MFC model. The study in this paper will be crucial to the further comprehension of MFC systems and has guiding significance for variety of fuel cells model.

ACKNOWLEDGMENTS

This work was financially supported by the National Natural Science Foundation of China (Grant: 61773226), the Key Research and Development Program of Shandong Province (Grant: 2018GGX103054, Grant: 2017GSF220005), and Independent Innovation Projects of Colleges and Universities in Jinan City (Grant: 201401210).

References

1. D. Pant, G.V. Bogaert, L. Diels, K. Vanbroekhoven, *Bioresour Technol*, 101 (2010) 1533-1543.
2. W. Hsiang-Yu, B. Angela, H. Chih-Yung, L. Duu-Jong, C. Jo-Shu, *Bioresource Technology*, 102 (2011) 235-243.
3. F. Ahmad, M.N. Atiyeh, B. Pereira, G.N. Stephanopoulos, *Biomass & Bioenergy*, 56 (2013) 179-188.
4. V.B. Oliveira, M. Simões, L.F. Melo, A.M.F.R. Pinto, *Biochemical Engineering Journal*, 73 (2013) 53-64.
5. I. Lee, G. Kim, S. Bang, A. Wolfe, R. Bell, S. Jeong, Y. Kim, J. Kagan, M. Arias-Thode, B. Chadwick, *IEEE Transactions on Circuits and Systems I: Regular Papers*, 62 (2015) 1126-1135.
6. I.A. Anderson, I.A. Ieropoulos, T. McKay, B. O'Brien, C. Melhuish, *IEEE/ASME Transactions on mechatronics*, 16 (2010) 107-111.
7. P.R. Bandyopadhyay, D.P. Thivierge, F.M. McNeilly, A. Fredette, *IEEE Journal of Oceanic Engineering*, 38 (2012) 32-42.
8. L. Na, R. Kakarla, B. Min, *International Journal of Hydrogen Energy*, 41 (2016) 20606-20614.
9. V. Margaria, T. Tommasi, S. Pentassuglia, V. Agostino, A. Sacco, C. Armato, A. Chiodoni, T. Schilirò, M. Quaglio, *International Journal of Hydrogen Energy*, 42 (2017) 1820-1829.
10. L.T. Angenent, K. Karim, M.H. Al-Dahhan, B.A. Wrenn, R. Domínguez-Espinosa, *TRENDS in Biotechnology*, 22 (2004) 477-485.
11. B.H. Kim, I.S. Chang, G.M. Gadd, *Applied Microbiology & Biotechnology*, 76 (2007) 485-494.
12. C.A. Pham, S.J. Jung, N.T. Phung, J. Lee, I.S. Chang, B.H. Kim, H. Yi, J. Chun, *FEMS Microbiology Letters*, 223 (2003) 129-134.
13. B.E. Logan, M. Cassandro, S. Keith, N.D. Gray, I.M. Head, *Water Research*, 39 (2005) 942-952.
14. L. Hong, B.E. Logan, *Environmental Science & Technology*, 38 (2004) 4040-4046.
15. J.K. Jang, T.H. Pham, I.S. Chang, K.H. Kang, H. Moon, K.S. Cho, B.H. Kim, *Process Biochemistry*, 39 (2004) 1007-1012.
16. R.P. Pinto, B. Tartakovsky, B. Srinivasan, *Journal of Process Control*, 22 (2012) 1079-1086.
17. R.P. Pinto, B. Srinivasan, M.F. Manuel, B. Tartakovsky, *Bioresour Technol*, 101 (2010) 5256-5265.
18. R.P. Pinto, B. Srinivasan, A. Escapa, B. Tartakovsky, *Environmental Science & Technology*, 45 (2011) 5039-5046.
19. M.D. Lorenzo, K. Scott, T.P. Curtis, I.M. Head, *Chemical Engineering Journal*, 156 (2010) 40-48.
20. H. Ren, C.I. Torres, P. Parameswaran, B.E. Rittmann, J. Chae, *Biosensors & Bioelectronics*, 61 (2014) 587-592.
21. S. Cheng, B.E. Logan, *Bioresource Technology*, 102 (2011) 4468-4473.
22. M.K. Alavijeh, M.M. Mardanpour, S. Yaghmaei, *Electrochimica Acta*, 167 (2015) 84-96.
23. S. Ou, Z. Yi, D.S. Aaron, J.M. Regan, M.M. Mench, *Journal of Power Sources*, 328 (2016) 385-396.

24. K.P. Katuri, K. Scott, *Enzyme & Microbial Technology*, 48 (2011) 351-358.
25. S. Cheng, D. Xing, B.E. Logan, *Biosensors and Bioelectronics*, 26 (2011) 1913-1917.
26. A.P. Borole, C.Y. Hamilton, T. Vishnivetskaya, *Biochemical Engineering Journal*, 48 (2009) 71-80.
27. C. Picioreanu, M.C.M. Loosdrecht, Van, K.P. Katuri, K. Scott, I.M. Head, *Water Science & Technology A Journal of the International Association on Water Pollution Research*, 57 (2008) 965.
28. P. Cristian, I.M. Head, K.P. Katuri, M.C.M. Loosdrecht, Van, S. Keith, *Water Research*, 41 (2007) 2921-2940.
29. G.-H. Song, H. Meng, *Acta Mechanica Sinica*, 29 (2013) 318-334.
30. A. Biyikoğlu, *International Journal of Hydrogen Energy*, 30 (2005) 1181-1212.
31. A. Saltelli, S. Tarantola, F. Campolongo, M. Ratto, *Chichester, England*, (2004).
32. J. Norton, *Environmental Modelling & Software*, 69 (2015) 166-174.
33. X.M. Song, J.Y. Zhang, C.S. Zhan, Y.Q. Xuan, M. Ye, C.G. Xu, *Journal of Hydrology*, 523 (2015) 739-757.
34. W.E. Thogmartin, *Ecological Modelling*, 221 (2010) 173-177.
35. B. Laoun, M.W. Naceur, A. Khellaf, A.M. Kannan, *International Journal of Hydrogen Energy*, 41 (2016) 9521-9528.
36. A. Saltelli, M. Ratto, T. Andres, F. Campolongo, J. Cariboni, D. Gatelli, M. Saisana, S. Tarantola, *Global sensitivity analysis: the primer*, John Wiley & Sons, 2008.
37. A. Saltelli, M. Ratto, S. Tarantola, F. Campolongo, *Chemical reviews*, 105 (2005) 2811-2828.
38. E. Borgonovo, *Reliability Engineering & System Safety*, 92 (2007) 771-784.
39. S.G. Perz, R. Muñoz-Carpena, G. Kiker, R.D. Holt, *Ecological Modelling*, 263 (2013) 174-186.
40. F. Ferretti, A. Saltelli, S. Tarantola, *Science of the Total Environment*, 568 (2016) 666-670.
41. L. Li, W. Fan, X. Jin, M.K.H. Leung, *Electrochimica Acta*, 187 (2015) 636-645.
42. G.N. Srinivasulu, T. Subrahmanyam, V.D. Rao, *International Journal of Hydrogen Energy*, 36 (2011) 14838-14844.
43. V. Griensven, MEIXNER, GRUNWALD, BISHOP, DILUZIO, *Journal of Hydrology*, 324 (2006) 10-23.
44. G. Baroni, S. Tarantola, *Environmental Modelling & Software*, 51 (2014) 26-34.
45. R. Salvador, J. Pinol, S. Tarantola, E. Pla, *Ecological Modelling*, 136 (2001) 0-189.
46. J. Nossent, P. Elsen, W. Bauwens, Sobol' sensitivity analysis of a complex environmental model, 2011.
47. K. Rabaey, J. Rodríguez, L.L. Blackall, J. Keller, P. Gross, D. Batstone, W. Verstraete, K.H. Nealson, *The ISME journal*, 1 (2007) 9.
48. Y. Zeng, Y.F. Choo, B.-H. Kim, P. Wu, *Journal of Power Sources*, 195 (2010) 79-89.
49. D. Hamby, *Environmental monitoring and assessment*, 32 (1994) 135-154.
50. L. Thabane, L. Mbuagbaw, S. Zhang, Z. Samaan, M. Marcucci, C. Ye, M. Thabane, L. Giangregorio, B. Dennis, D. Kosa, *Bmc Medical Research Methodology*, 13 (2013) 92-92.
51. I. Dimov, R. Georgieva, *Mathematics and Computers in Simulation*, 81 (2010) 506-514.
52. I.M. Sobol, *Mathematical modelling and computational experiments*, 1 (1993) 407-414.
53. T. Homma, A. Saltelli, *Reliability Eng.syst.safety*, 52 (1996) 1-17.
54. A. Saltelli, P. Annoni, I. Azzini, F. Campolongo, M. Ratto, S. Tarantola, *Computer Physics Communications*, 181 (2010) 259-270.
55. I.M. Sobol, B.V. Shukman, *Mathematical & Computer Modelling*, 18 (1993) 39-45.
56. A.M. An, Y.L. Liu, H.C. Zhang, C.D. Zheng, J. Fu, *CIESC Journal*, 68 (2017) 1090-1098.